International Journal of Chemical Studies

P-ISSN2349–8528
E-ISSN 2321–4902
IJCS 2016; 4(5): 123-127

Received: 18-07-2016
Accepted: 19-08-2016

P Babji
Department of Physical, Nuclear Chemistry & Chemical Oceanography, School of Chemistry, Andhra University, Visakhapatnam, Andhra Pradesh, India

V Lakshmana Rao
Department of Physical, Nuclear Chemistry & Chemical Oceanography, School of Chemistry, Andhra University, Visakhapatnam, Andhra Pradesh, India

Correspondence
P Babji
Department of Physical, Nuclear Chemistry & Chemical Oceanography, School of Chemistry, Andhra University, Visakhapatnam, Andhra Pradesh, India

Catalytic reduction of 4-Nitrophenol to 4-Aminophenol by using Fe_2O_3-Cu_2O-TiO_2 nanocomposite

P Babji and V Lakshmana Rao

Abstract
In this work, a simple sol-gel method was used to synthesize magnetic Fe_2O_3-Cu_2O-TiO_2 nanocomposite by using sol gel method and their application for the catalytic reduction of 4-nitrophenol to 4-aminophenol by using reductant as $NaBH_4$. The synthesized catalyst was characterized by XRD, FT-IR, FE-SEM and EDS have been applied to investigate the structure and morphology of the Fe_2O_3-Cu_2O-TiO_2 nanocomposite. The obtained catalyst showed best catalytic ability than pure TiO_2. Since the magnetic nanocomposites are readily recovered from the solution phase without centrifugation or filtration. The Fe_2O_3-Cu_2O-TiO_2 nanocomposite was synthesized in this work has been exploited as solid phase catalysts for the reduction of 4-nitrophenol in the presence of $NaBH_4$.

Keywords: TiO_2, Fe_2O_3-Cu_2O-TiO_2, 4-nitrophenol, $NaBH_4$

1. Introduction
Nitrophenols are very important organic compounds, but they cause deleterious effects in biological systems due to their acute toxicity in water and soil. The biological treatment of pollutants provided more safe and effective method as compared with the chemical treatment techniques including activated carbon adsorption, chemical oxidation, etc. However, the problems in the biological treatment of pollutants are the slow reaction rate and difficulty to find the suitable microorganism.

Nitrophenol (NP) is a water pollutant with high toxicity, which is of great environmental concern [1, 2]. Hence, there is an urgent need for solving such an environmental problem. The resistance of the NP compound to chemical oxidation, biological oxidation, and hydrolysis is due to the electron-withdrawing effect of the nitro group. Among the processes contributing to the remediation of nitrophenol, reduction of the nitro group is certainly the most characteristic. Many processes have been developed for the NP removal such as adsorption, microbial degradation, photocatalytic degradation, microwave-assisted catalytic oxidation, the electro-Fenton method, electrocoagulation, and electrochemical treatment [3-9]. Metallic nanoparticles have been the subject of intense research during recent years because of their potential use in catalysis [10-13].

PNP, as with other nitrophenols and derivatives, is a common byproduct from the production of pesticides, herbicides, and synthetic dyes [14]. Many noble metal alloy nanoparticles are reported for the treatment of water but application of transition metal particles (monometallic and bimetallic alloy particles) is very limited in the literature [15-21]. PNP is easily reduced by $NaBH_4$ in the presence of metals in solution [22-23].

One would then suppose that both the activity and the selectivity of suspended catalysts could benefit much from the use of small-sized supports. The separation of solid catalysts from the reaction products simply by filtration or centrifugation necessitates, however, that the catalyst bodies are larger than about 3 μm: Smaller bodies are difficult to be separated out. It is thus highly necessary to develop new catalysts with a nanometer-sized magnetic core and a catalytic shell, which respectively favor the high surface area and convenient magnetic separation. Magnetically recyclable nanometer-sized catalysts allow the catalysts to be recycled conveniently through applying an external magnetic field. Many attempts have been made to synthesize this kind of noble-metal deposited magnetic materials (Fe_3O_4, c-Fe_2O_3, etc.) [24-27].

In order to investigate the catalytic activity of the magnetic Fe_2O_3-Cu_2O-TiO_2 nanocomposite, we have chosen the reduction of 4-nitrophenol by $NaBH_4$ as a model reaction. 4-Aminophenol finds its application as a photographic developer, corrosion inhibitor, dyeing agent etc [2]. In this investigation, we choose copper (Cu) and maghemite (γ-Fe_2O_3) nanoparticles as the functional components to construct the magnetically recyclable nanometer-sized catalysts. The Fe_2O_3-Cu_2O-TiO_2 nanocomposite are in fact found to be efficient nanocatalysts for the reduction of 4-nitrophenol.

2. Experimental Procedure

2.1 Materials and Reagents

Nano iron (III) oxide (Spherical, less than diameter 50nm, 99.5%) was purchased from Sigma Aldrich Chemical Co., Ltd., USA. Ammonia solution, isopropyl alcohol and anhydrous ethanol were obtained from Hangzhou High-crystal Fine Chemical Co., Ltd., China. Copper Nitrate, Tetrabutyl titanate (TBOT), 4-Nitro Phenol and Sodium borohydride were purchased from Merck, China.

2.2 Synthesis of Fe_2O_3-Cu_2O-TiO_2 nanocomposite.

The 0.25g of Fe_2O_3 nanoparticles were ultra sonicated for 1h to make them uniformly dispersed in anhydrous ethanol (40mL). Concentrated ammonium hydroxide (4.5mL) was diluted to the above solution and 0.75g of Copper Nitrate were quickly added under vigorous stirring. The solution was left to stirred for 12h. The product was washed with anhydrous ethanol three times. The resultant product was redispersed in anhydrous ethanol (40mL). Subsequently, a proper amount of TBOT(5.0mL) dissolved in isopropyl alcohol (40.0mL) was introduced to the system drop wise, followed by heating the solution at about 70 ºC. The whole process was under vigorous stirred for 12h, after that reddish brown precipitates were washed with deionized water and ethanol five times and dried in a vacuum oven at 80 ºC for 24h. Finally, the products were calcined in air at 500 ºC for 2h. An un-doped TiO_2 (anatase) sample was also prepared by adopting the above procedure without adding the Fe_2O_3 nanoparticles and copper nitrate which is pure TiO_2.

2.3 Catalyst characterization

Crystalline structure and crystallinity of the Fe_2O_3-Cu_2O-TiO_2 nanocomposite were examined using an X-ray Diffractometer (Shimadzu, XRD-6000) equipped with Cu Kα radiation source using Ni as filter at a setting of 45 kV/40 mA. A 2θ scan range from 10 to 90 ºC, a scanning step size of 0.01 ºC and a scintillation counter detector was used. Curve fitting and integration was carried out using proprietary software from Philips X'Pert high score plus. Fourier transform infrared (FT-IR) spectroscopy was carried for a Fe_2O_3-Cu_2O-TiO_2 nanocomposite was obtained in the range 4,000 to 500 cm^{-1} with an IR-Prestige-21 Shimadzu FT-IR spectrophotometer, by KBr pellet method. The FE-SEM micrographs were obtained using a JEOL 6335F FE-SEM microscope equipped with a Thermo Noran energy dispersive spectroscopy (EDS) detector. The presence of elemental Iron, Copper, Titanium and Oxygen was confirmed through EDAX. The EDAX observations were carried out in STIC, CUSAT, (JOEL Model JED-2300).

3. Results and Discussion

3.1 X-ray Diffraction

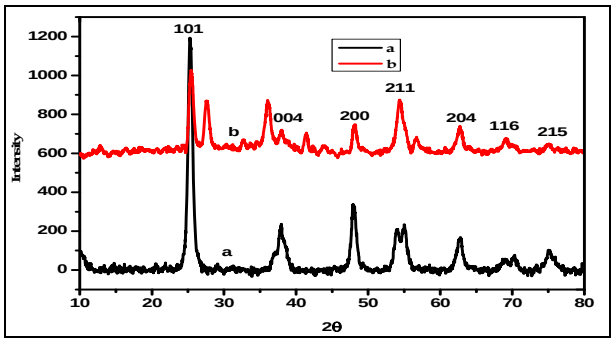

Fig 1: XRD patterns of un-doped TiO_2 (a), and Fe_2O_3-Cu_2O-TiO_2 nanocomposite (b).

Fig. 1 shows the XRD patterns of un-doped TiO_2 (curve a), and Fe_2O_3-Cu_2O-TiO_2 nanocomposite (curve b) powders. It is found that all of the crystal phase is anatase for all of the samples [28]. The shape of the diffraction peaks of all the photo catalysts was consistent with that of un-doped TiO_2. The well-defined diffraction peaks with 2θ are at about 25°, 38°, 48°, 54°, 62°, 70° and 74° which are assigned to the (101), (004), (200), (211), (204) (116), (220) and (215) crystal planes, respectively. This XRD characteristic pattern is consistent with the standard JCPDS values of anatase TiO_2 (JCPDS Card No. 21-1272) [29-30] with tetragonal structure and did not appear in rutile and brookite form.

3.2 Fourier Transform Infrared Spectroscopy

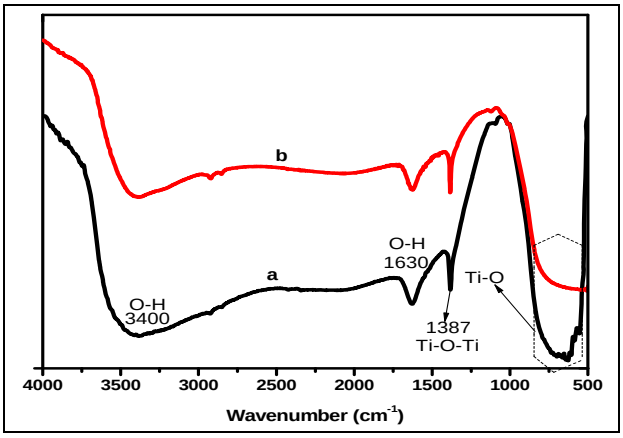

Fig 2: FT-IR spectra of Un-doped TiO_2 (a), and (b) Fe_2O_3-Cu_2O-TiO_2 nanocomposite.

The FTIR spectra of the all samples in the frequency range of 500–4000 cm^{-1} are shown in Fig. 2. All the samples show peaks corresponding to the stretching vibration of O–H and bending vibrations of adsorbed water molecules around 3200–3400 cm^{-1} and 1600 cm^{-1} respectively [28, 31-32]. Furthermore, the broadening of ~3400cm^{-1} O-H stretching vibration the formation of a different -OH group, and most probably as Ti-OH surface group. The broad intense band in the range of 450–700 cm^{-1} is due to the Ti–O stretching and Ti–O–Ti bridging stretching modes [29-30]. Fe_2O_3-Cu_2O-TiO_2 nanocomposite intensity has reduced compared to un-doped TiO_2.

3.3 Field Emission-Scanning Electron Microscopic Study

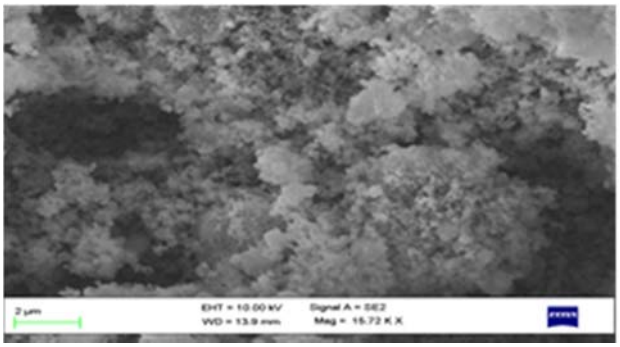

a)

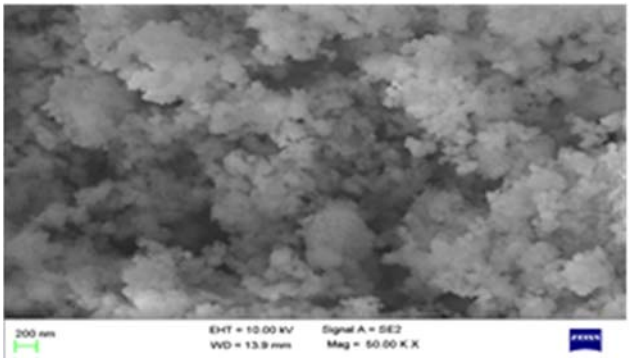

b)

Fig 3: FE-SEM images of Fe_2O_3-Cu_2O-TiO_2 nanocomposite.

The morphology and structure of the Fe_2O_3-Cu_2O-TiO_2 nanocomposite of synthesized samples were investigated by field emission scanning electron microscopy (FE-SEM). The FE-SEM images of samples at different magnification are shown in figure 3. (a) and (b) respectively. According to the FE-SEM, the morphology of the Fe_2O_3-Cu_2O-TiO_2 nanocomposite were observed and approximately spherical, in which the Fe and Cu deposited with titanium dioxide nanoparticles were in aggregated form. This reveals that the powder particles are slightly agglomerated and the closed view of spherical nanoparticles has showed in Fig. 3a and b.

3.4 Energy Dispersive X-ray (EDX) spectra

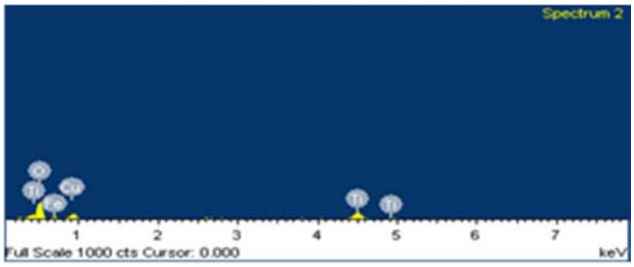

Fig 4: EDS spectra of Fe_2O_3-Cu_2O-TiO_2 nanocomposite.

The energy dispersive X-ray (EDX) spectra of the Fe_2O_3-Cu_2O-TiO_2 nanocomposite are shown in Fig.4 respectively. The peaks corresponding to titanium, oxygen and the respective deposited metals of Iron and Copper can be confirmed by fig 4.

4. Catalytic reduction of 4-nitrophenol to 4-aminophenol

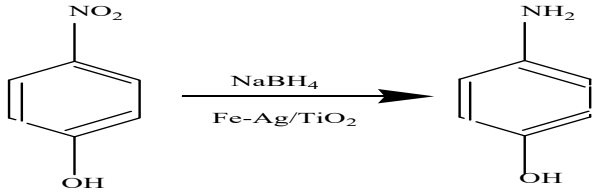

P-Nitro Phenol P-Amino Phenol

Scheme 1: Schematic representation of the performance of Fe_2O_3-Cu_2O-TiO_2 nanocomposite as catalysts in the reduction of 4-nitrophenol to 4-aminophenol by $NaBH_4$.

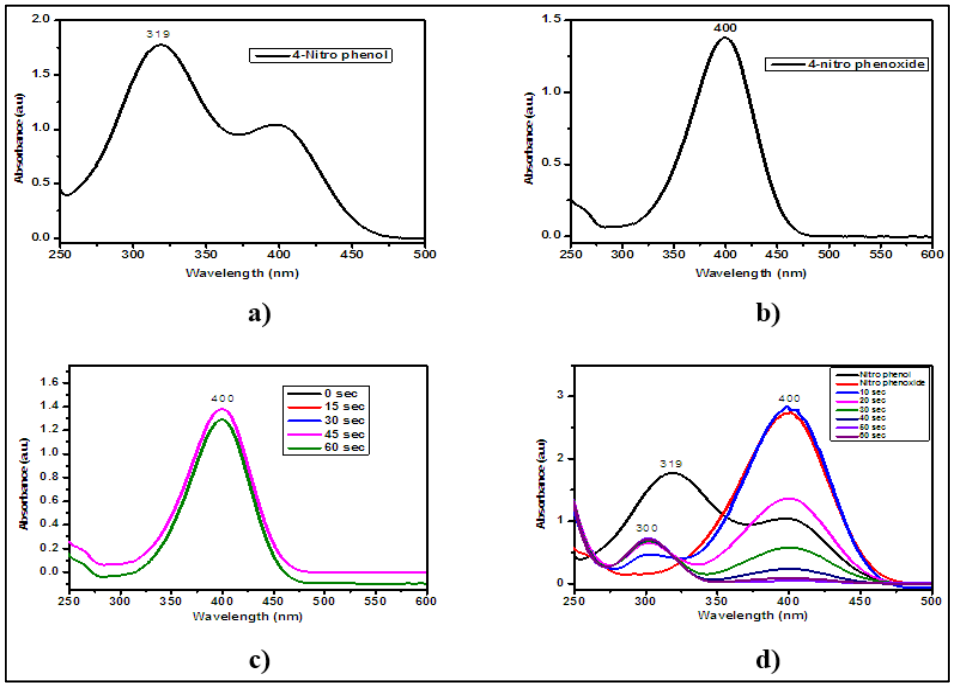

Fig 5: gives UV-Vis absorption spectra of 4-nitrophenol taken (a) before, (b) after immediate addition of $NaBH_4$, (c) un-doped TiO_2 and (d) Fe_2O_3-Cu_2O-TiO_2 nanocomposite.

4.1 Catalytic Activity of Fe_2O_3-Cu_2O-TiO_2 nanocomposite

Recently, several research groups have investigated the catalytic reduction of 4-nitrophenol with $NaBH_4$, using a number of noble metals Ag, Au, Cu, Pt, and Pd nanoparticles [22, 33-39] in different substrates such as dendrimers, polyelectrolytes, biological cells, and so on [22, 40-41]. Before we investigate the catalytic activity of the Fe_2O_3-Cu_2O-TiO_2 nanocomposite, the catalytic ability of the pure TiO_2 nanoparticles was examined. An aqueous solution of 4-nitrophenol (1.5mmol in 100mL) has a maximum absorption at 319 nm, as shown by a trace in Fig. 5a. But it has been observed that, after immediate addition of freshly prepared aqueous solution of $NaBH_4$, the peak due to 4-nitrophenol was red shifted from 319 to 400 nm (see Fig. 5b). This peak was due to the formation of 4-nitrophenolate ions in alkaline condition caused by the addition of $NaBH_4$ [36]. In the absence of proper catalyst, the thermodynamically favorable reduction of 4-nitrophenol (the standard reduction potentials for 4-nitrophenol/4-aminophenol and H_3BO_3/BH_4- are -0.76 and -1.33 V, respectively) was not observed and the peak due to 4-nitrophenol ions at 400 nm remains unaltered even a couple of days as reported in the literatures [22, 38]. Under alkaline conditions, the decomposition of borohydride is much slower. Borohydride is relatively environmentally friendly because of the low toxicity of borates. The advantage of the catalytic reduction of 4-NP is the easy monitoring of the reactant 4-nitrophenolate anion (λ_{max}=400nm) through spectro-photometry. The 4-nitrophenolate anion formation from 4-NP (pKa= 7.15) in the initial step upon addition of borohydride is indicated when the peak at 319 nm (due to 4-NP) is shifted to 400 nm. The sole product 4-AP (λ_{max}=300 nm) can also be monitored easily, and when required to know whether the reduction is actually taking place. Under certain situations, a significant decrease in absorbance at 400 nm may not be associated with the concomitant evolution of a peak at 300 nm indicating that the process does not involve any reduction, rather it is a mere adsorption of the nitro phenolate ion [41]. The UV–vis absorption spectrum after the addition of pure TiO_2 nanoparticles in the mixture of 4-nitrophenol and $NaBH_4$ also remains unaltered with time, as shown in Fig. 5c, which means that the pure TiO_2 nanoparticles do not work as catalyst for this reaction.

The addition of small amount of Fe_2O_3-Cu_2O-TiO_2 nanocomposite, however, causes fading and ultimate bleaching of the yellow color of the reaction mixture. As shown in Fig. 5d, time dependent UV–vis spectra of this catalytic reaction mixture display the disappearance of 400 nm peak and the gradual development of the new peak at 300 nm which substantiates the formation of the 4-aminophenol [42]. These results indicate that Fe_2O_3-Cu_2O-TiO_2 nanocomposite indeed catalyze the reduction process.

In this experiment, the concentration of the borohydride ion, used as reductant, largely exceeds (50 times) that of 4-nitrophenol. As soon as we added the $NaBH_4$, the Fe_2O_3-Cu_2O-TiO_2 nanocomposite started the catalytic reduction by relaying electrons from the donor BH_4^- to the acceptor 4-nitrophenol right after the adsorption of both onto the particle surfaces. As the initial concentration of Sodium borohydride was very high, it remained essentially constant throughout the reaction.

The Fe_2O_3-Cu_2O-TiO_2 nanocomposite are very effective for the catalytic reduction of 4-nitrophenol. At the end of the reaction, the catalyst particles remained active and were easily separated from the product, 4-aminophenol, using an external magnet.

5. Conclusions

The catalytic performance of Fe_2O_3-Cu_2O-TiO_2 nanocomposite for the reduction of 4- NP to 4-AP was tested as a model reaction with an excess amount of $NaBH_4$. Accordingly, the reduction rates can be regarded as being independent of the concentration of $NaBH_4$. After adding $NaBH_4$ into the aqueous solution of 4-NP, the color of the solution changed from light yellow to dark yellow due to the formation of 4-nitrophenolate ion. Then, the color of the 4-nitrophenolate ions faded with time after the addition of Fe_2O_3-Cu_2O-TiO_2 nanocomposite. The progress of the reaction could be monitored by UV–Vis spectroscopy. The characteristic peak of 4-NP at 400 nm decreased, while at 300nm a new peak appeared which were assigned to 4-AP. The reaction was finished within 60s at room temperature. The reaction did not proceed in this period in the absence of Fe_2O_3-Cu_2O-TiO_2 nanocomposite or with un-doped TiO_2 alone.

6. References

1. Panigrahi S, Basu S, Praharaj S, Pande S, Jana S, Pal A *et al.* Synthesis and Size-Selective Catalysis by Supported Gold Nanoparticles: Study on Heterogeneous and Homogeneous Catalytic Process. J Phys Chem C. 2007; 111(12):4596-4605.
2. Vaidya MJ, Kulkarni SM, Chaudhari RV. Synthesis of p-Aminophenol by Catalytic Hydrogenation of p-Nitrophenol. Org Process Res Dev. 2003; 7(2):202-208.
3. Marais E, Nyokong T. Adsorption of 4-nitrophenol onto Amberlite® IRA-900 modified with metallophthalocyanines. J Hazard Mater. 2008; 152(1):293-301.
4. O'Connor OA, Young LY. Toxicity and anaerobic biodegradability of substituted phenols under methanogenic conditions. Environ Toxicol Chem. 1989; 8(10):853-862.
5. Dieckmann MS, Gray KA. A comparison of the degradation of 4-nitrophenol via direct and sensitized photocatalysis in TiO_2 slurries. Water Res. 1996; 30(5):1169-1183.
6. Bo LL, Zhang YB, Quan X, Zhao B. Microwave assisted catalytic oxidation of p-nitrophenol in aqueous solution using carbon-supported copper catalyst. J Hazard Mater. 2008; 153(3):1201-1206.
7. Oturan MA, Peiroten J, Chartrin P, Acher AJ. Complete Destruction of p-Nitrophenol in Aqueous Medium by Electro-Fenton Method. Environ Sci Technol. 2000; 34(16):3474-3479.
8. Modirshahla N, Behnajady MA, Mohammadi-Aghdam S. Investigation of the effect of different electrodes and their connections on the removal efficiency of 4-Nitrophenol from aqueous solution by electrocoagulation. J Hazard Mater. 2008; 154(1-3):778-786.
9. Canizares P, Sez C, Lobato J, Rodrigo MA. Electrochemical Treatment of 4-Nitrophenol Containing Aqueous Wastes Using Boron-Doped Diamond Anodes. Ind Eng Chem Res. 2004; 43(9):1944-1951.
10. Astruc D. Nanoparticles and Catalysis. Wiley-VCH. New York. 2008.
11. Narayanan R, El-Sayed MA. Catalysis with Transition Metal Nanoparticles in Colloidal Solution: Nanoparticle Shape Dependence and Stability. J Phys Chem B. 2005; 109(26):12663-12676.
12. Hashmi AS, Hutchlings GJ. Gold Catalysis. Angew Chem Int Ed. 2006; 45(47):7896-7936.

13. Astruc D, Lu F, Aranzaes JR. Nanoparticles as Recyclable Catalysts: The Frontier between Homogeneous and Heterogeneous Catalysis. Angew Chem Int Ed. 2005; 44(48):7852-7872.
14. Vincent T, Guibal E. Chitosan Supported Palladium Catalyst. 3. Influence of Experimental Parameters on Nitrophenol Degradation. Langmuir. 2003; 19(20):8475-8483.
15. Shin KS, Choi JY, Park CS, Jang HJ, Kim K. Facile Synthesis and Catalytic Application of Silver-Deposited Magnetic Nanoparticles. Catal Lett. 2009; 133:1-7.
16. Comisso N, Cattarin S, Fiameni S, Gerbasi R, Mattarozzi L, Musiani M *et al.* Electrodeposition of Cu–Rh alloys and their use as cathodes for nitrate reduction. Electrochem Commun. 2012; 25:91-93.
17. Narayanan KB, Sakthivel N. Synthesis and characterization of nano-gold composite using Cylindrocladium floridanum and its heterogeneous catalysis in the degradation of 4-nitrophenol. J Hazard Mater. 2011; 189(1-2):519-525.
18. Lai TL, Yong KF, Yu JW, Chen JH, Shu YY, Wang CB. High efficiency degradation of 4-nitrophenol by microwave-enhanced catalytic method. J Hazard Mater. 2011; 185(1):366-372.
19. Makovec D, Sajko M, Selišnik A, Drofenik M. Magnetically recoverable photocatalytic nanocomposite particles for water treatment. Mater Chem Phys. 2011; 129(1-2):83-89.
20. Zhang W, Tan F, Wang W, Qiu X, Qiao X, Chen J. Facile, template-free synthesis of silver nanodendrites with high catalytic activity for the reduction of p-nitrophenol. J Hazard Mater. 2012, 217-218, 36-42.
21. Lu W, Ning R, Qin X, Zhang Y, Chang G, Liu S *et al.* Synthesis of Au nanoparticles decorated graphene oxide nanosheets: Noncovalent functionalization by TWEEN 20 in situ reduction of aqueous chloroaurate ions for hydrazine detection and catalytic reduction of 4-nitrophenol. J Hazard Mater. 2011; 197:320-326.
22. Hayakawa K, Yoshimura T, Esumi K. Preparation of Gold-Dendrimer Nanocomposites by Laser Irradiation and their Catalytic Reduction of 4- Nitrophenol. Langmuir. 2003; 19(13):5517-5521,
23. Kuroda K, Ishida T, Haruta M. Reduction of 4-Nitrophenol to 4-Aminophenol Over Au Nanoparticles Deposited on PMMA. J Mol Catal A Chem. 2009; 298(1-2):7-11.
24. Caruntu D, Cushing BL, Caruntu G, O'Connor CJ. Attachment of Gold Nanograins onto Colloidal Magnetite Nanocrystals. Chem Mater. 2005; 17(13):3398-3402.
25. Bao J, Chen W, Liu T, Zhu Y, Jin P, Wang L *et al.* Bifunctional Au-Fe_3O_4 Nanoparticles for Protein Separation. Acs Nano. 2007; 1(4):293-298.
26. Zhang DH, Li GD, Li JX, Chen JS. One-pot synthesis of Ag-Fe_3O_4 nanocomposite: a magnetically recyclable and efficient catalyst for epoxidation of styrene. Chem Commun. 2008; 29:3414-3416.
27. Zhang L, Dou YH, Gu HC. Synthesis of Ag–Fe_3O_4 heterodimeric nanoparticles. J Colloid Interf Sci. 2006; 297(2):660-664.
28. Venkatachalam N, Palanichamy M, Murugesan V. Sol–gel preparation and characterization of alkaline earth metal doped nano TiO_2: Efficient photocatalytic degradation of 4-chlorophenol. J Mol Catal A: Chem. 2007; 273(1-2):177-185.
29. Tao J, Shen Y, Gu F, Zhu J, Zhang J. Synthesis and Characterization of Mesoporous Titania Particles and Thin Films. J Mater Sci Technol. 2007; 23:513-516.
30. Jagadale TC, Takale SP, Sonawane RS, Joshi HM, Patil SI, Kale BB *et al.* N-Doped TiO_2 nanoparticle based Visible Light Photocatalyst by modified Peroxide Sol-Gel Method. J Phys Chem C. 2008; 112(37):14595-14602.
31. Venkatachalam N, Palanichamy M, Arabindoo B, Murugesan V. Enhanced photocatalytic degradation of 4-chlorophenol by Zr^{4+} doped nano TiO_2. J Mol Catal A: Chem. 2007; 266(1-2):158-165.
32. Chen X, Wang X, Fu X. Hierarchical macro/mesoporous TiO_2/SiO_2 and TiO_2/ZrO_2 nanocomposites for environmental photocatalysis. Energy Environ Sci. 2009; 2(8):872-877.
33. Pradhan N, Pal A, Pal T. Silver nanoparticle catalyzed reduction of aromatic nitro compounds. Colloids Surf. A. 2002; 196(2-3):247-257.
34. Esumi K, Isono R, Yoshimura T. Preparation of PAMAM and PPI-Metal (Silver, Platinum, and Palladium) Nanocomposites and their Catalytic Activities for Reduction of 4-Nitrophenol. Langmuir. 2004; 20(1):237-243.
35. Praharaj S, Nath S, Ghosh SK, Kundu S, Pal T. Immobilization and Recovery of Au Nanoparticles from Anion Exchange Resin: Resin-Bound Nanoparticle Matrix as a Catalyst for the Reduction of 4-Nitrophenol. Langmuir. 2004; 20(23):9889-9892.
36. Jana S, Ghosh SK, Nath S, Pande S, Praharaj S, Panigrahi S *et al.* Synthesis of silver nanoshell-coated cationic polystyrene beads: A solid phase catalyst for the reduction of 4-nitrophenol. Appl Catal A: Gen. 2006; 313(1):41-48.
37. Rashid MdH, Bhattacharjee RR, Kotal A, Mandal TK. Synthesis of Spongy Gold Nanocrystals with Pronounced Catalytic Activities. Langmuir. 2006; 22(17):7141-7143.
38. Chen X, Zhao D, An Y, Zhang Y, Cheng J, Wang B *et al.* Formation and catalytic activity of spherical composites with surfaces coated with gold nanoparticles. J Colloid Interf Sci. 2008; 322(2):414-420.
39. Ge J, Huynh T, Hu Y, Yin Y. Hierarchical Magnetite/Silica Nanoassemblies as Magnetically Recoverable Catalyst–Supports. Nano Lett. 2008; 8(3):931-934.
40. Mei Y, Sharma G, Lu Y, Ballauff M, Drechsler M, Irrgang T *et al.* High Catalytic Activity of Platinum Nanoparticles Immobilized on Spherical Polyelectrolyte Brushes. Langmuir. 2005; 21(26):12229-12234.
41. Sharma NC, Sahi SV, Nath S, Parsons JG, Gardea-Torresde JL, Pal T. Synthesis of Plant-Mediated Gold Nanoparticles and Catalytic Role of Biomatrix-Embedded Nanomaterials. Environ Sci Technol. 2007; 41(14):5137-5142.
42. Ghosh SK, Mandal M, Kundu S, Nath S, Pal T. Bimetallic Pt–Ni nanoparticles can catalyze reduction of aromatic nitro compounds by Sodium borohydride in aqueous solution. Appl Catal A: Gen. 2004; 268(1-2):61-66.